nature neuroscience

Oxytocin mediates early experience–dependent cross-modal plasticity in the sensory cortices

Jing-Jing Zheng[1–3], Shu-Jing Li[1,3], Xiao-Di Zhang[1,2], Wan-Ying Miao[1], Dinghong Zhang[1,2], Haishan Yao[1] & Xiang Yu[1]

Sensory experience is critical to development and plasticity of neural circuits. Here we report a new form of plasticity in neonatal mice, where early sensory experience cross-modally regulates development of all sensory cortices via oxytocin signaling. Unimodal sensory deprivation from birth through whisker deprivation or dark rearing reduced excitatory synaptic transmission in the correspondent sensory cortex and cross-modally in other sensory cortices. Sensory experience regulated synthesis and secretion of the neuropeptide oxytocin as well as its level in the cortex. Both *in vivo* oxytocin injection and increased sensory experience elevated excitatory synaptic transmission in multiple sensory cortices and significantly rescued the effects of sensory deprivation. Together, these results identify a new function for oxytocin in promoting cross-modal, experience-dependent cortical development. This link between sensory experience and oxytocin is particularly relevant to autism, where hypersensitivity or hyposensitivity to sensory inputs is prevalent and oxytocin is a hotly debated potential therapy.

During the early postnatal period, neural activity, both in the form of spontaneous electrical activity and sensory stimulation, is critical to the formation of functional neural circuits[1–3]. A large body of work using unimodal sensory deprivation manipulations has shown that depriving the appropriate inputs during early development reduced responsiveness in the corresponding cortical region[4–8]. Conversely, increased sensory experience through environmental enrichment elevates such responses[9–11]. Multiple synaptic mechanisms contribute to experience-dependent plasticity in primary sensory cortices[12].

In addition to inducing changes in the target sensory cortex, sensory experience also cross-modally affects other brain regions[13–16]. Studies in humans have shown that deprivation of one sense, such as blindness, results in enhanced function of the remaining senses, including superior performance in discrimination of auditory pitch, better spatial localization of sound and/or finer tactile-discrimination thresholds[13–16]. Relatively little is known about the synaptic mechanisms underlying cross-modal plasticity[17–19]. In previous studies, the animals underwent normal sensory experience before initiation of the deprivation protocol, which leaves open the question of what cross-modal plasticity mechanisms are used during the very beginning of neural-circuit development, before the onset of sensory experience. This question is especially important because individuals sensory deprived from early life generally have better cross-modal compensations in other sensory modalities[13,15,16], suggesting that the mechanisms of cross-modal plasticity altered over time. A better understanding of the molecular mechanisms underlying cross-modal plasticity during early development would not only contribute to our understanding of plasticity mechanisms in individuals subjected to sensory deprivation from birth, such as the congenitally blind or deaf, but also that of individuals with hypersensitivity or hyposensitivity to sensory inputs, prevalent among children diagnosed with autism spectrum disorders (ASD)[20,21].

To examine the cross-modal effects of early sensory deprivation, we removed whiskers from mice at birth and examined the effect of whisker deprivation both in the target primary somatosensory cortex (S1) and in other sensory cortices, including the primary visual cortex (V1) and the primary auditory cortex (Au1). Recording from layer II/III pyramidal neurons, we found that whisker deprivation reduced excitatory synaptic transmission and neuronal excitability in S1 and cross-modally in V1 and Au1. We observed similar cross-modal effects after deprivation of visual inputs through rearing mice in the dark (dark rearing). Whisker deprivation also cross-modally reduced V1 responses to flash stimuli *in vivo*. We also found that firing rates of hypothalamic neurons that secrete the neuropeptide oxytocin, the synthesis and secretion of oxytocin in the hypothalamus, as well as the level of cortical oxytocin peptide, were all reduced after sensory deprivation. *In vivo*, oxytocin injection elevated excitatory synaptic transmission and rescued the effect of whisker deprivation in both S1 and V1. Conversely, sequestering endogenous oxytocin or interfering with its signaling reduced excitatory synaptic transmission. Finally, enhanced sensory stimulation through environmental enrichment increased the level of oxytocin, elevated excitatory synaptic transmission in multiple sensory cortices and rescued the effects of sensory deprivation. Together, these results identify a new function for oxytocin signaling in promoting cross-modal, experience-dependent cortical development.

[1]Institute of Neuroscience and State Key Laboratory of Neuroscience, Shanghai Institutes for Biological Sciences, Chinese Academy of Sciences, Shanghai, China. [2]University of Chinese Academy of Sciences, Shanghai, China. [3]These authors contributed equally to this work. Correspondence should be addressed to X.Y. (yuxiang@ion.ac.cn).

Received 17 September 2013; accepted 9 December 2013; published online 26 January 2014; doi:10.1038/nn.3634

RESULTS

Cross-modal effect of sensory deprivation in sensory cortex

Because somatosensory stimuli are likely to be predominant sensory inputs in mice during early postnatal development, we whisker-deprived mice by removing all whiskers on both sides of the face from postnatal day 0 (P0) to P14, which spans the window of maximal synaptogenesis in the cerebral cortex[22]. As compared to recordings from control littermates with intact whiskers, whole-cell recordings from layer II/III pyramidal neurons of the S1 barrel field of whisker-deprived mice showed significantly lower frequencies of miniature excitatory postsynaptic currents (mEPSCs), with no changes in their amplitudes (**Fig. 1a–c**). Spontaneous neuronal firing rates were also significantly reduced (**Fig. 1d,e**), whereas inhibitory synaptic transmission, as measured by the frequencies and amplitudes of miniature inhibitory postsynaptic currents (mIPSCs), was not significantly affected (**Supplementary Fig. 1a–c**).

To examine whether cross-modal effects can be detected in other sensory cortices at this early developmental stage, we recorded from layer II/III pyramidal neurons of other sensory cortices. In V1 of whisker-deprived mice, we found significantly reduced mEPSC frequencies and slight but significantly increased mEPSC amplitudes compared to littermates with intact whiskers (**Fig. 1f–h**). Spontaneous firing rates were significantly reduced in V1 (**Fig. 1i,j**), but mIPSCs were not affected (**Supplementary Fig. 1d–f**). We also observed cross-modal reduction in mEPSC frequencies and spontaneous firing rates in Au1 (**Fig. 1k,l**). But we observed no significant changes in the prefrontal cortex (PFC) (**Fig. 1k,l**), which demonstrates that the cross-modal effect was specific to sensory cortices.

Consistent with the reduction in excitatory synaptic transmission, in whisker-deprived mice we observed significantly lower amount of glutamate receptors, including the AMPA receptor (AMPAR) subunit GRIA2 and the NMDA receptor (NMDAR) subunit GRIN2B, in S1 and cross-modally in V1 (**Fig. 1m**). We detected significantly reduced mEPSC frequencies in whisker-deprived mice as early as P7, in both S1 and V1 (**Supplementary Fig. 1g,h**).

To determine whether such cross-modal effect can be observed *in vivo* in response to sensory stimulation, we examined visually evoked responses of V1 neurons in control and whisker-deprived mice. By measuring responses to light spots flashed at different positions in the visual field, we found that both the firing rates and the signal-to-noise ratios of V1 responses were significantly reduced in whisker-deprived mice (**Fig. 2**). These results indicate that deprivation of somatosensory stimulation cross-modally caused substantial impairment of V1 responses to visual stimuli.

To explore whether this cross-modal effect of sensory experience was a general phenomenon, we used a dark-rearing protocol, another

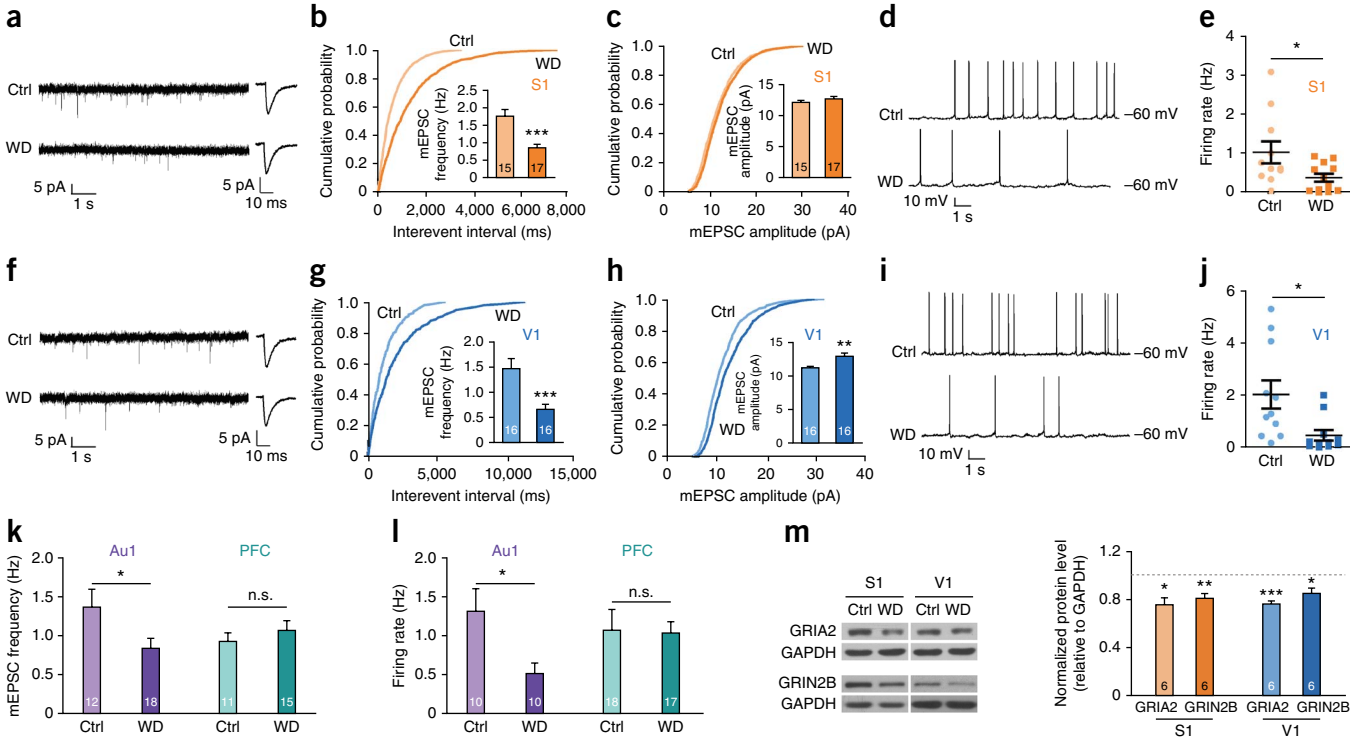

Figure 1 Whisker deprivation from birth significantly reduced excitatory synaptic transmission in layer II/III pyramidal neurons of the S1 barrel field and cross-modally in other sensory cortices. (**a**,**f**) Representative mEPSC recordings (left) and average waveforms (right) for whisker-deprivation (WD) condition and control (Ctrl) from S1 (**a**) and V1 (**f**). (**b**,**c**) mEPSC frequencies (**b**, bar graphs: $P < 0.001$; cumulative distributions: $P < 0.001$) and mEPSC amplitudes (**c**, bar graphs: $P = 0.33$; cumulative distributions: $P = 0.42$) in S1 at P14. (**d**,**i**) Representative spontaneous firing recordings for conditions as indicated in S1 (**d**) and V1 (**i**). (**e**) Spontaneous firing rates in S1 ($P = 0.034$) at P14. (**g**,**h**) mEPSC frequencies (**g**, bar graphs: $P < 0.001$; cumulative distributions: $P < 0.001$) and mEPSC amplitudes (**h**, bar graphs: $P = 0.006$; cumulative distributions: $P = 0.024$) in V1. (**j**) Spontaneous firing rates in V1 ($P = 0.014$). (**k**) mEPSC frequencies in Au1 ($P = 0.037$) and PFC ($P = 0.44$). (**l**) Spontaneous firing rates in Au1 ($P = 0.023$) and PFC ($P = 0.91$). (**m**) Representative immunoblots and quantitation of GRIA2 and GRIN2B levels from S1 and V1 of whisker-deprived mice, normalized to that of control mice (GRIA2, S1, $P = 0.011$, V1, $P = 0.0002$; GRIN2B, S1, $P = 0.0052$, V1, $P = 0.020$). Error bars, s.e.m.; *n* values denoted inside bar graphs represent the number of neurons, except for immunoblots where they represent number of mice. $^*P < 0.05$, $^{**}P < 0.01$, $^{***}P < 0.001$, n.s., not significant, using unpaired two-tailed Student's *t*-tests for bar graphs and Kolmogorov-Smirnov two-sample tests for cumulative distributions in electrophysiology experiments and paired *t*-tests for immunoblots. Means and s.e.m. are presented in **Supplementary Table 1**. Full-length immunoblots are presented in **Supplementary Figure 8**.

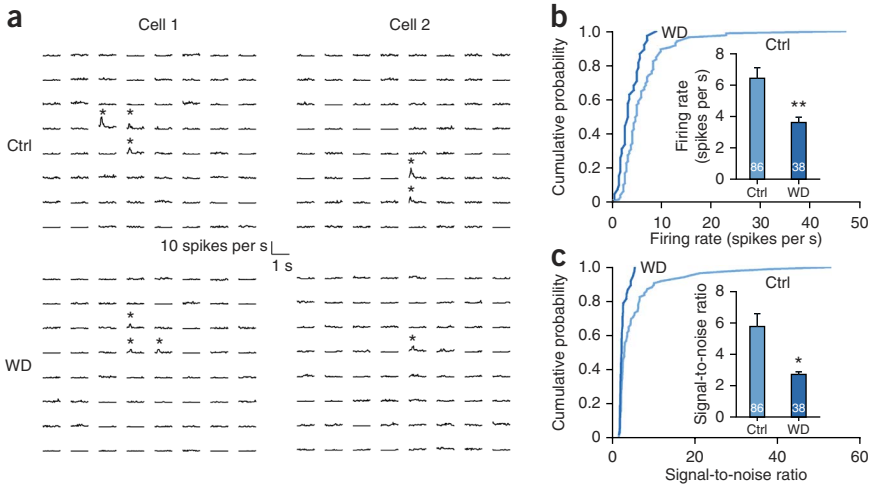

Figure 2 Whisker deprivation from birth significantly reduced visually evoked responses for neurons in V1. (**a**) Spike receptive fields for two V1 cells in control mice (Ctrl) and two V1 cells in whisker-deprived mice (WD). Each trace represents the averaged response to light squares flashed at each of 64 positions on an 8 × 8 grid. Asterisks mark traces with significant visual responses evoked by flash stimuli. (**b**) Firing rates in V1 (bar graphs: $P = 0.0052$, two-tailed unpaired *t*-test; cumulative distributions: $P = 0.0048$, Kolmogorov-Smirnov two-sample test). (**c**) Signal-to-noise ratio in V1 (bar graphs: $P = 0.016$, two-tailed unpaired *t*-test; cumulative distributions: $P = 0.0057$, Kolmogorov-Smirnov two-sample test). $^*P < 0.05$, $^{**}P < 0.01$. Error bars, s.e.m.; *n* values denoted inside bar graphs represent the number of neurons.

well-established unimodal sensory deprivation mainipulation. Rearing mice in the dark from birth effectively reduced mEPSC frequencies in V1, and cross-modally in S1 and Au1, but not in the PFC (**Fig. 3a–c**). Dark rearing of mice also significantly reduced neuronal firing in V1 and cross-modally in S1 (**Fig. 3d,e**). In both V1 and S1 of dark-reared mice we detected a reduced level of GRIA2 and GRIN2B (**Fig. 3f**). We observed a reduction in mEPSC frequencies in dark-reared mice in both S1 and V1 as early as P7 (**Supplementary Fig. 1i,j**). Thus, using whisker deprivation and dark rearing, two independent unimodal sensory-deprivation manipulations, we observed cross-modal effects of sensory deprivation on reducing excitatory synaptic transmission in multiple sensory cortices (**Figs. 1** and **3**).

Sensory deprivation reduced oxytocin expression

What might be the molecular mechanism underlying this early form of experience-dependent cross-modal plasticity? We surmised that it could be either due to postsynaptic changes in the sensory cortices or induced by a small diffusible molecule secreted elsewhere. Using microarrays to screen for changes in gene expression, in an unbiased fashion, between control and dark-reared mice at P14, we found no correlated changes in S1 and V1. In contrast, in samples containing both thalamic and hypothalamic regions, we observed differences in the amounts of mRNA encoding several neuropeptides between control and dark-reared mice (**Supplementary Fig. 2a**). Testing samples from additional litters of whisker-deprived and dark-reared mice, we found that only the amount of mRNA encoding the neuropeptide oxytocin was consistently reduced under both deprivation manipulations (**Fig. 4a** and **Supplementary Fig. 2b,c**).

Oxytocin is a neuropeptide synthesized in the paraventricular (PVN) and supraoptic (SON) nuclei of the hypothalamus. Initially identified for its role in lactation and parturition, oxytocin is important in the regulation of social emotional behaviors in mammals[23–25]. It has recently received much attention as a potential 'prosocial hormone' and as a hotly debated therapy for treating children with ASD[23,24,26–28]. No previous role of oxytocin in early cortical development has been described.

Consistent with the reduced amount of oxytocin mRNA in the hypothalamus of sensory-deprived mice (**Fig. 4a**), we found a significantly reduced number of oxytocin-positive neurons in the PVN of these mice (**Fig. 4b–d** and **Supplementary Fig. 3a**; we confirmed specificity of oxytocin antibody by colocalization with its carrier protein Neurophysin I (refs. 24,25), **Supplementary Fig. 3b**). This change was specific to the PVN, as the number of oxytocin neurons in the SON was not affected (**Fig. 4b–d**). To determine whether neuronal death has occurred, we performed terminal deoxynucleotidyl transferase dUTP nick-end labeling (TUNEL) in P14 sensory-deprived mice and observed no apoptosis at this time point (**Supplementary Fig. 3c–e**). Lower oxytocin synthesis in the PVN was translated into

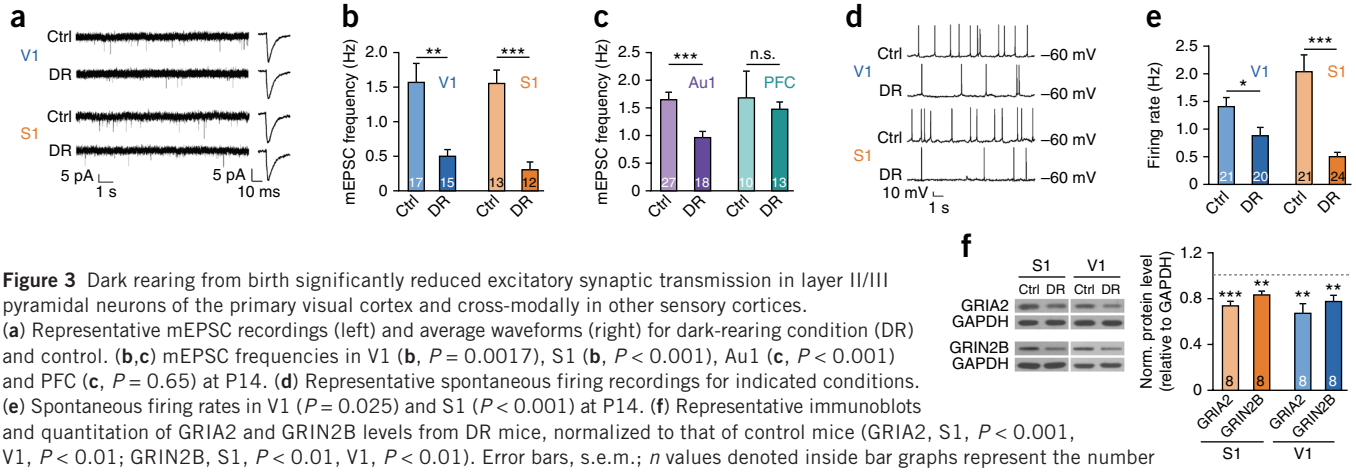

Figure 3 Dark rearing from birth significantly reduced excitatory synaptic transmission in layer II/III pyramidal neurons of the primary visual cortex and cross-modally in other sensory cortices. (**a**) Representative mEPSC recordings (left) and average waveforms (right) for dark-rearing condition (DR) and control. (**b**,**c**) mEPSC frequencies in V1 (**b**, $P = 0.0017$), S1 (**b**, $P < 0.001$), Au1 (**c**, $P < 0.001$) and PFC (**c**, $P = 0.65$) at P14. (**d**) Representative spontaneous firing recordings for indicated conditions. (**e**) Spontaneous firing rates in V1 ($P = 0.025$) and S1 ($P < 0.001$) at P14. (**f**) Representative immunoblots and quantitation of GRIA2 and GRIN2B levels from DR mice, normalized to that of control mice (GRIA2, S1, $P < 0.001$, V1, $P < 0.01$; GRIN2B, S1, $P < 0.01$, V1, $P < 0.01$). Error bars, s.e.m.; *n* values denoted inside bar graphs represent the number of neurons, except for immunoblots *n* values represent number of mice. $^*P < 0.05$, $^{**}P < 0.01$, $^{***}P < 0.001$, using unpaired two-tailed Student's *t*-tests for electrophysiology experiments and paired *t*-tests for immunoblots. Full-length immunoblots are presented in **Supplementary Figure 8**.

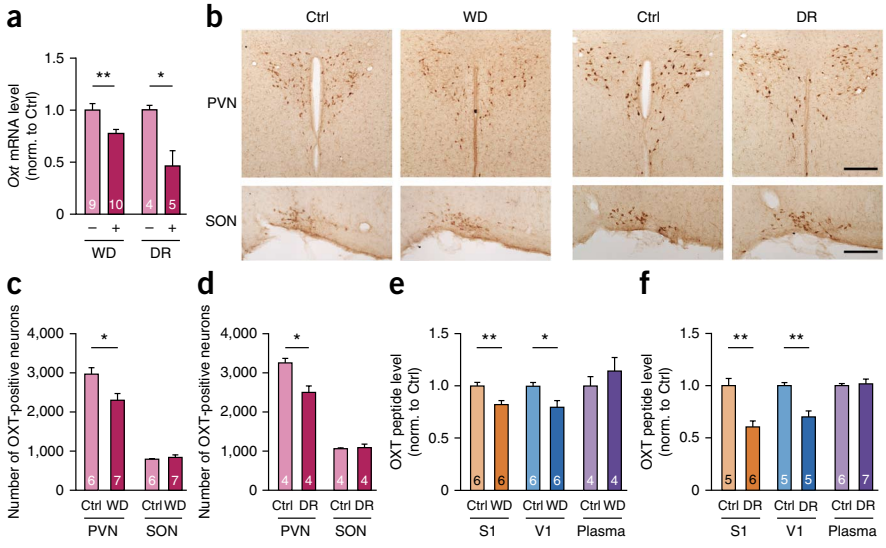

Figure 4 Sensory deprivation from birth reduced oxytocin level at P14. (**a**) Oxytocin mRNA level in the hypothalamus in mice not subjected to (–) and subjected to (+) whisker deprivation (WD; $P = 0.007$) or dark rearing (DR; $P = 0.018$). (**b**) Representative images of oxytocin-positive neurons in the PVN and SON of P14 mice, conditions as indicated. Scale bars, 200 µm. (**c**) Number of oxytocin-positive neurons in the PVN ($P = 0.018$) and SON ($P = 0.67$) of whisker-deprived mice. (**d**) Number of oxytocin-positive neurons in the PVN ($P = 0.010$) and SON ($P = 0.62$) of dark-reared mice. (**e**) Oxytocin peptide level in S1 ($P = 0.006$), V1 ($P = 0.02$) and plasma ($P = 0.39$) of whisker-deprived mice compared to controls. (**f**) Oxytocin peptide level in S1 ($P = 0.003$), V1 ($P = 0.003$) and plasma ($P = 0.79$) of dark-reared mice compared to controls. Error bars, s.e.m.; *n* values denoted inside bar graphs represent the number of mice. $*P < 0.05$, $**P < 0.01$, $***P < 0.001$, using unpaired two-tailed Student's *t*-test.

reduced amount of oxytocin peptide in S1 and V1 under both sensory-deprivation protocols (**Fig. 4e**,**f**), which demonstrated that cortical oxytocin peptide level is regulated by sensory experience.

Sensory deprivation reduced oxytocin release from the PVN

We next asked whether sensory deprivation affected the activity of oxytocin neurons in the PVN. We labeled oxytocin neurons in the PVN by stereotaxically injecting a recombinant adeno-associated virus (AAV) expressing Venus under the oxytocin promoter[29] (see **Supplementary Fig. 3f** for specificity of virus). Recording from acute PVN slices of P14–P15 mice, we found that the spontaneous firing rates of oxytocin neurons was significantly reduced in whisker-deprived mice (**Fig. 5a**,**b**), demonstrating that the activity of PVN oxytocin neurons is regulated by sensory experience.

We next asked whether sensory deprivation also affected oxytocin secretion. We measured oxytocin peptide level in the incubation medium of acute PVN brain slices, which contained mostly the soma and dendrites of oxytocin neurons, together with local and centrally projecting axons. Oxytocin release from the PVN was significantly reduced in sensory-deprived mice (**Fig. 5c**). Oxytocin has been shown to be released at high levels from dendrites[30–32] and to travel to other brain regions either via diffusion or through cerebrospinal fluid (CSF)[32,33]. The proximity of the PVN to the third ventricle provides easy access of locally released oxytocin to the CSF[30–33] as a high density of oxytocin-containing fibers run along the ventricular surface of the third ventricle (**Supplementary Fig. 3g**). Consistently, we detected significantly less oxytocin peptide in the CSF of sensory-deprived mice (**Fig. 5d**). Furthermore, injection of oxytocin antibody (OXT-Ab, 1 µg) into the lateral ventricles to sequester endogenous diffusible oxytocin significantly reduced mEPSC frequencies in both S1 and V1 (**Fig. 5e**), supporting the CSF as a likely mode for oxytocin to reach the cerebral cortex. This result demonstrates the requirement for oxytocin in mediating cross-modal plasticity during early development.

In addition to local secretion from the PVN region, oxytocin is also released from the axon terminals of long-range projections. The axons of most oxytocin neurons terminate in the posterior pituitary, where oxytocin is released into the peripheral blood circulation. Some axons also project centrally to a number of brain regions. Previous studies using adult mice did not identify direct projections from the PVN to sensory cortex[25]. We investigated this possibility in young mice by injecting the retrograde tracer Cholera toxin subunit B into the S1 region of P9 mice. We successfully labeled known projections

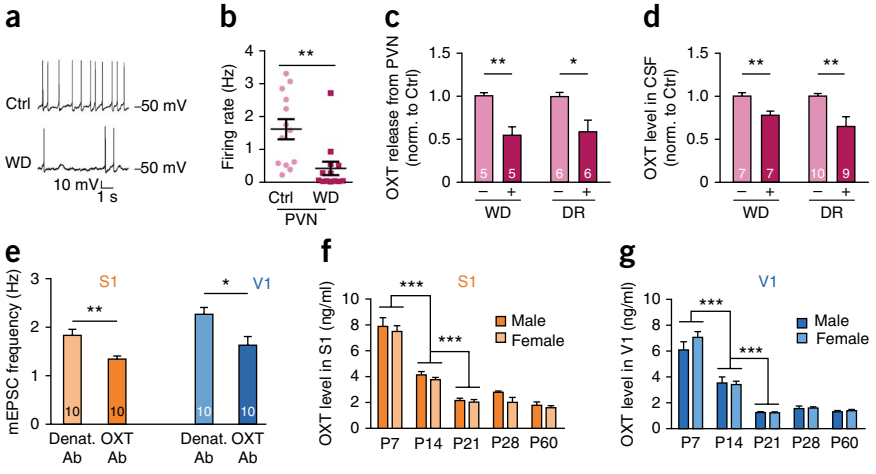

Figure 5 Sensory deprivation from birth reduced oxytocin release. (**a**) Representative spontaneous firing recordings for whisker-deprived condition (WD) and control. (**b**) Spontaneous firing rates in oxytocin-expressing neurons in the PVN ($P = 0.0035$). (**c**) Oxytocin release in the PVN of whisker-deprived ($P = 0.003$) and dark-reared (DR; $P = 0.016$) mice compared to controls (–). (**d**) Oxytocin peptide level in the CSF of whisker-deprived ($P = 0.006$) and dark-reared ($P = 0.007$) mice compared to controls (–). (**e**) Injection of oxytocin antibody (OXT Ab) into the ventricle reduced mEPSC frequencies in S1 ($P = 0.003$) and V1 ($P = 0.013$). Denat., denatured. (**f**,**g**) Developmental expression profile of oxytocin peptide in S1 (**f**, $P < 0.001$) and V1 (**g**, $P < 0.001$); $n = 3$ mice per gender per age group; $P < 0.001$ between the P7 and P14, as well as between the P14 and P21 groups using one-way analysis of variance (ANOVA). Error bars, s.e.m.; *n* values denoted inside bar graphs represent the number of mice, except for **b**,**e**, where they represent the number of neurons. $*P < 0.05$, $**P < 0.01$, $***P < 0.001$, using unpaired two-tailed Student's *t*-test, unless otherwise specified.

to S1, from both the thalamus and the contralateral cerebral cortex (**Supplementary Fig. 4**) at P14, but did not detect projections from the PVN or SON. As a control, we retrogradely labeled previously described projections from the PVN to the central medial amygdala[29] (**Supplementary Fig. 5**). We excluded the blood circulation possibility because sensory deprivation did not affect the plasma oxytocin level (**Fig. 4e**,**f**). Furthermore, during development of the mouse, the reduction in the amount of oxytocin peptide in S1 and V1 (**Fig. 5f**,**g**) was very distinct from the increase in the amount of oxytocin mRNA in the hypothalamus and the increase in the amount of oxytocin peptide in the plasma (**Supplementary Fig. 6a**,**b**). These differences, together with the reported inability of oxytocin to cross the blood-brain barrier[34], make blood circulation an unlikely route.

Regulation of synaptic transmission by oxytocin signaling

We next asked whether oxytocin was necessary and sufficient for regulating excitatory synaptic transmission. Recording mEPSCs in acute brain slices prepared from homozygous oxytocin knockout ($Oxt^{-/-}$) mice[35], we found significantly reduced mEPSC frequencies in S1 layer II/III pyramidal neurons at P14, as compared to wild-type littermates (**Fig. 6a**,**b**). This result demonstrates a requirement for oxytocin in promoting excitatory synaptic transmission during sensory cortical development.

In the sufficiency experiment, bath application of oxytocin (1 μM) onto acute cortical slices of wild-type mice significantly increased mEPSC frequencies of S1 layer II/III pyramidal neurons, whereas prior application of the denatured peptide onto the same cell had no such effect (**Fig. 6c**,**d**). This effect of oxytocin was concentration-dependent and specific to developing mice (**Supplementary Fig. 6c**,**d**). Application of oxytocin did not significantly affect mEPSC frequencies in the PFC (**Fig. 6e**), suggesting that the lack of changes in PFC layer II/III pyramidal neurons after sensory deprivation (**Fig. 1k**,**l**) was due to the inability of these cells to respond to oxytocin at P14. Consistently, the amount of oxytocin receptor (*Oxtr*) mRNA was significantly lower in the PFC as compared to S1 and V1 at P14 (**Supplementary Fig. 6e**).

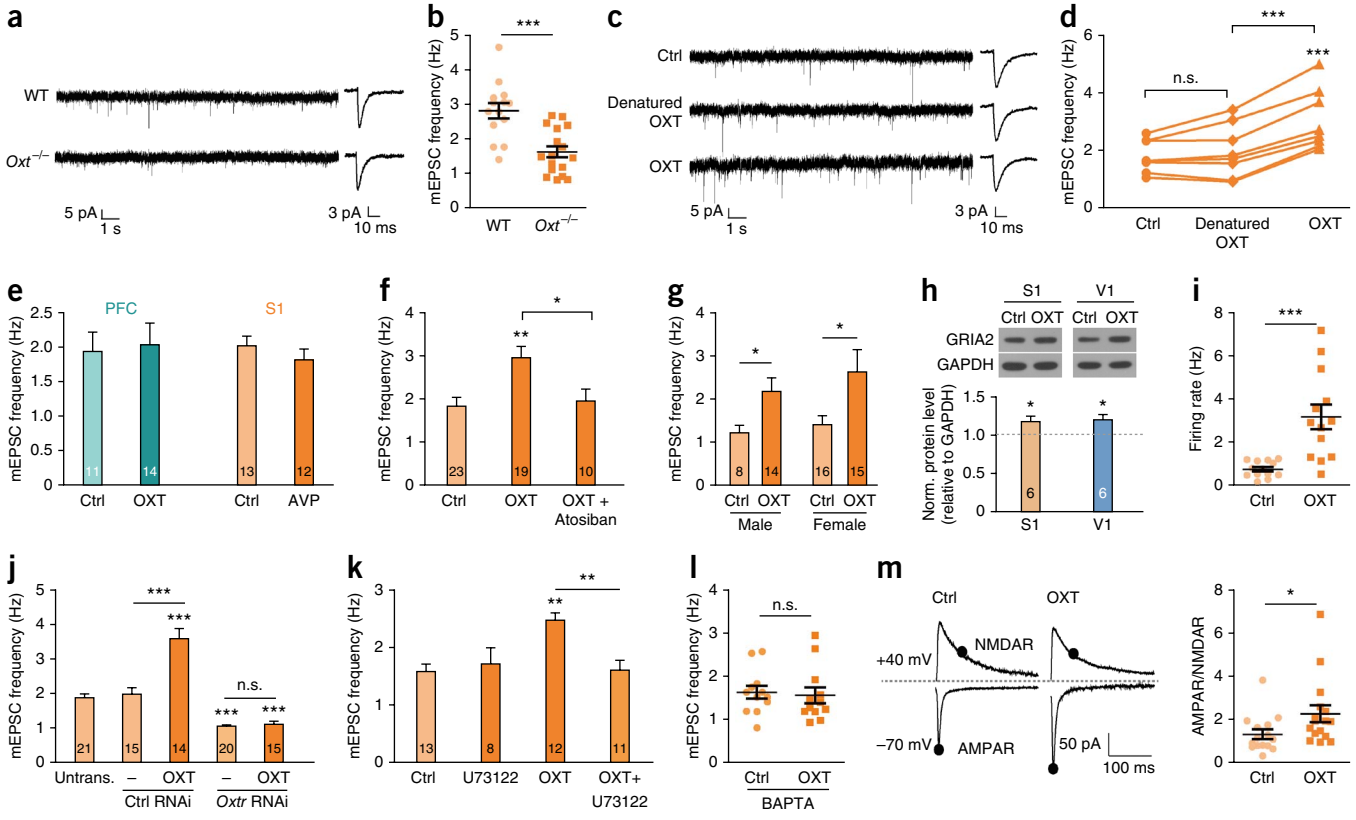

Figure 6 Oxytocin application significantly increased excitatory synaptic transmission in S1 layer II/III pyramidal neurons via OXTR-mediated signaling. (**a**) Representative mEPSC recordings (left) and average waveforms (right) for wild-type (WT) and $Oxt^{-/-}$ mice. (**b**) mEPSC frequencies in S1 ($P < 0.001$). (**c**) mEPSC traces (left) and average waveforms (right) from a single neuron during application of regular extracellular solution (control), followed by solution containing denatured oxytocin (OXT) and then OXT. (**d**) Bath application of oxytocin increased mEPSC frequencies, but prior application of denatured OXT to the same cells had no such effect ($P < 0.001$, repeated measures ANOVA). (**e**) Effect of oxytocin application on mEPSC frequencies in the PFC ($P = 0.80$) and of vasopressin (AVP) application on mEPSC frequencies in S1 ($P = 0.36$). (**f**) Coapplication of atosiban prevented the effect of oxytocin in increasing mEPSC frequencies ($P < 0.01$, one-way ANOVA). (**g**) Effect of *in vivo* oxytocin injection on mEPSC frequencies in male ($P = 0.046$) and female ($P = 0.035$) mice. (**h**) Representative immunoblots and quantitation of GRIA2 level from sensory cortices of mice 24 h after injection of oxytocin, normalized to that of control littermates (S1, $P = 0.046$, V1, $P = 0.032$, paired *t*-tests). (**i**) Spontaneous firing rates after oxytocin injection ($P < 0.001$). (**j**) RNAi of *Oxtr* prevented the effect of oxytocin in increasing mEPSC frequencies ($P < 0.0001$, one-way ANOVA). (**k**) mEPSC frequencies in cells treated with phospholipase C inhibitor U73122 and oxytocin as indicated compared to control ($P < 0.01$, one-way ANOVA). (**l**) mEPSC frequencies of neurons treated with OXT, recorded with intracellular solution containing BAPTA ($P = 0.78$). (**m**) Left, representative recordings of AMPAR- and NMDAR-mediated responses in conditions as indicated; filled circles indicate time points at which measurements were taken; right, effect of bath application of oxytocin on AMPAR/NMDAR ratio ($P = 0.047$). Error bars, s.e.m.; *n* values denoted inside bar graphs represent the number of neurons, except for immunoblots *n* values represent number of mice. $^*P < 0.05$, $^{**}P < 0.01$, $^{***}P < 0.001$, n.s., not significant, using unpaired two-tailed Student's *t*-tests, unless otherwise specified. Full-length immunoblots are presented in **Supplementary Figure 8**.

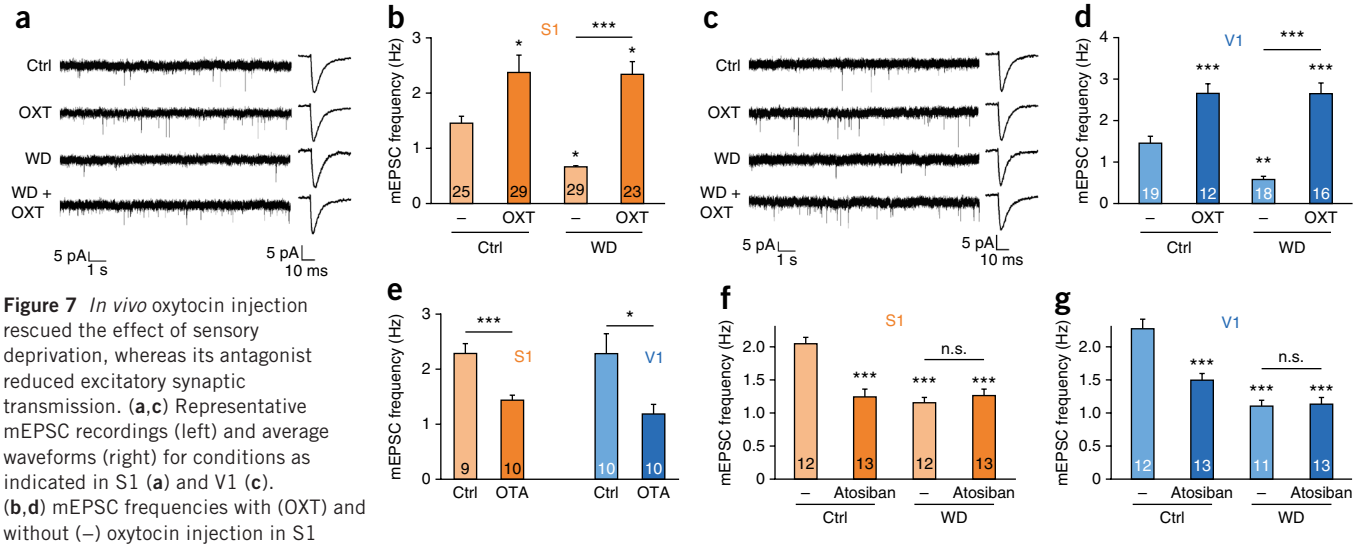

Figure 7 *In vivo* oxytocin injection rescued the effect of sensory deprivation, whereas its antagonist reduced excitatory synaptic transmission. (**a**,**c**) Representative mEPSC recordings (left) and average waveforms (right) for conditions as indicated in S1 (**a**) and V1 (**c**). (**b**,**d**) mEPSC frequencies with (OXT) and without (–) oxytocin injection in S1 (**b**, $P < 0.001$) and V1 (**d**, $P < 0.001$) of mice subjected to whisker deprivation and control mice. (**e**) mEPSC frequencies upon injection of oxytocin receptor antagonist OTA, in S1 ($P < 0.001$) and V1 ($P = 0.015$). (**f**,**g**) mEPSC frequencies upon injection of atosiban in mice treated as indicated, in S1 (**f**, $P < 0.001$) and V1 (**g**, $P < 0.001$). Error bars, s.e.m.; *n* values denoted inside bar graphs represent the number of neurons. n.s., not significant; $*P < 0.05$, $**P < 0.01$, $***P < 0.001$, using unpaired two-tailed Student's *t*-tests for sample pairs and one-way ANOVA followed by Tukey's multiple-comparison tests for groups of three or more samples.

The effect of oxytocin in promoting excitatory synaptic transmission in the sensory cortex was specific, as application of the related neuropeptide vasopressin did not significantly alter excitatory synaptic transmission (**Fig. 6e**). Furthermore, the effect of oxytocin on increasing mEPSC frequencies was effectively blocked by application of its receptor antagonist atosiban (**Fig. 6f**).

To assay the *in vivo* effect of oxytocin, we injected 1 ng of oxytocin into the S1 of P12/13 mice and performed electrophysiological recordings from acute cortical slices cut 1 d later. We observed significant increases in mEPSC frequencies in both male and female mice (**Fig. 6g**), suggesting no gender differences in oxytocin response at this early developmental stage. The increase in excitatory synaptic transmission was accompanied by significant increase in the level of GRIA2 (**Fig. 6h**), and by increased neuronal firing (**Fig. 6i**).

The oxytocin signal is mediated through OXTR, a G protein–coupled receptor widely expressed throughout the brain and at high levels in the forebrain and hypothalamus[33,36–38]. In the cerebral cortex, *Oxtr* mRNA level has been reported to be high in the superficial layers and to gradually decrease in the deeper layers[33,38]. Lowering endogenous OXTR level in layer II/III pyramidal neurons using RNA interference (RNAi) with a lentivirus expressing *Oxtr* short interfering (si)RNA (see **Supplementary Fig. 6f** for efficiency; injected at P9) significantly reduced mEPSC frequencies by P14 and completely blocked the effect of acute oxytocin application, whereas RNAi with a control siRNA had no such effect (**Fig. 6j**). This result demonstrates that postsynaptic OXTR-mediated signaling is required for oxytocin-dependent regulation of mEPSCs.

OXTR belong to the $G_{q/11}$ subclass of G protein–coupled receptors, which signal through activation of phospholipase C and inositol triphosphate–triggered calcium release from intracellular stores[36]. We demonstrated that these downstream signaling mechanisms are involved in OXTR-mediated signaling, as either bath application of the phospholipase C inhibitor U73122 (10 μM) or intracellular loading of the calcium chelator BAPTA (5 mM) completely blocked the effect of oxytocin application on increasing mEPSC frequencies (**Fig. 6k**,**l**). The lack of changes in paired-pulse ratios (**Supplementary Fig. 6g**,**h**) and significant increase in AMPAR/NMDAR ratios upon application of oxytocin (**Fig. 6m**) provided additional evidence for the postsynaptic effect of oxytocin.

Cross-modal rescue by oxytocin and enriched environment

If oxytocin functioned downstream of sensory experience, one would expect oxytocin application to rescue the effects of sensory deprivation. Indeed, we found that *in vivo* injection of oxytocin into S1 24 h before electrophysiological recordings fully rescued the reduction in mEPSC frequencies induced by whisker deprivation in both S1 and V1 (**Fig. 7a–d**). Consistently, *in vivo* injection of oxytocin receptor antagonists OTA ($(d(CH_2)_5^1,Tyr(Me)^2,Thr^4,Orn^8,des\text{-}Gly\text{-}NH_2^9)$-vasotocin; 200 ng) or atosiban (200 ng) to the lateral ventricles significantly reduced mEPSC frequencies in both S1 and V1 (**Fig. 7e–g**), demonstrating a role for endogenous oxytocin signaling in the development of excitatory synaptic transmission. *In vivo* injection of atosiban did not further reduce mEPSC frequencies in whisker-deprived mice (**Fig. 7f**,**g**), supporting the notion that the effect of sensory deprivation in reducing mEPSC frequencies in multiple sensory cortices is primarily mediated via oxytocin and its receptors.

We next asked whether increased sensory experience promoted oxytocin signaling *in vivo*. In previous work, we established a protocol for environmental enrichment from birth, in which we stimulated neonatal mice through multiple sensory modalities, including increased tactile, olfactory, visual and motor stimuli[39] (**Supplementary Fig. 7a**). Rearing mice from birth until P14 in an enriched environment effectively elevated oxytocin mRNA level in the hypothalamus and oxytocin peptide level in S1 and V1 (**Fig. 8a**,**b**). Furthermore, 'enrichment' significantly increased mEPSC frequencies in both S1 and V1 (**Fig. 8c–f**), an effect opposite to that of sensory deprivation. Enrichment significantly rescued the effect of whisker deprivation or dark rearing in both S1 and V1, restoring mEPSC frequencies to a level significantly above that of deprivation alone (**Fig. 8c–f**). In the whisker-deprivation manipulation, because the control mice are littermates of the whisker-deprived mice under both standard and enriched conditions, changes in the pups, rather than their mothers, are necessary and sufficient for experience-dependent cross-modal changes in excitatory synaptic transmission.

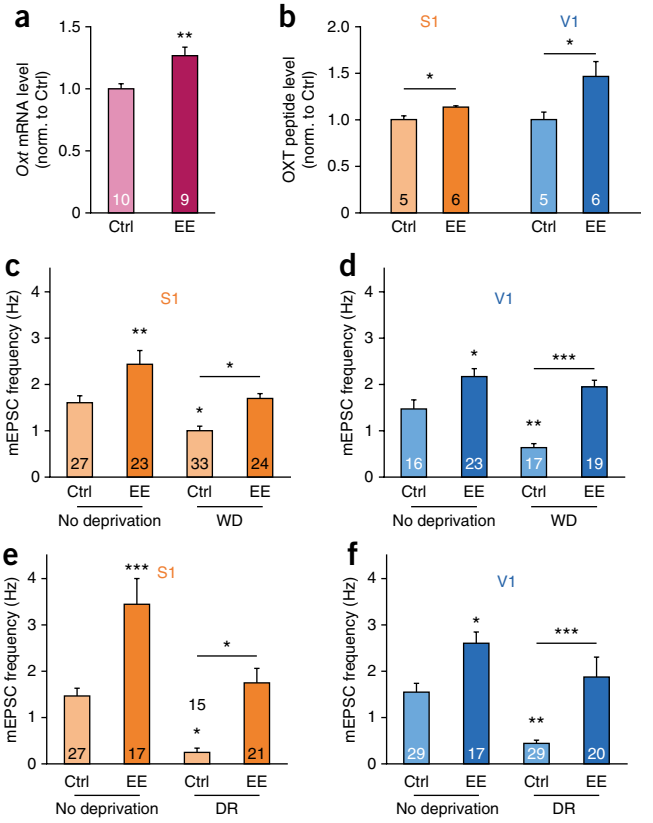

Figure 8 Environmental enrichment rescued the effect of sensory deprivation. (**a**,**b**) Effect of environmental enrichment (EE) on oxytocin mRNA level in the hypothalamus ($P = 0.0027$) (**a**) and on oxytocin peptide level in S1 ($P = 0.024$) and V1 ($P = 0.042$) (**b**). (**c**,**d**) Effect of enrichment on mice subjected to whisker deprivation, in S1 (**c**, $P < 0.001$) and V1 (**d**, $P < 0.001$). (**e**,**f**) Effect of enrichment on mice subjected to dark rearing, in S1 (**e**, $P < 0.001$) and V1 (**f**, $P < 0.001$). Error bars, s.e.m.; *n* values denoted inside bar graphs represent the number of neurons. (**c**–**f**) and the number of mice (**a**,**b**). $*P < 0.05$, $**P < 0.01$, $***P < 0.001$, using unpaired two-tailed Student's *t*-tests for sample pairs and one-way ANOVA followed by Tukey's multiple comparison tests for groups of three or more samples.

DISCUSSION

We described a new form of oxytocin-mediated experience-dependent cross-modal plasticity during early development, in which sensory experiences from multiple modalities work together to promote excitatory synaptic transmission in the sensory cortices. We identified a role for oxytocin in regulating excitatory synaptic transmission in the sensory cortices, at a much earlier developmental stage than the previously described roles of oxytocin in mediating social emotional behaviors[23–25].

Early experience–dependent cross-modal plasticity

Sensory experience, especially interaction with the environment, is critical to development of the sensory cortices[1–11]. Extensive neuronal morphogenesis and synapse formation occur during the first few years of human brain development[40], a process that takes place over the first few postnatal weeks in rodents[22]. We identified a new form of experience-dependent cross-modal plasticity within this window of maximal synaptogenesis. We found that deprivation of inputs to one modality not only reduced excitatory synaptic transmission in the target sensory cortex but also acted cross-modally in other sensory cortices. Whisker deprivation resulted in significantly impaired V1 responses to flash stimuli, demonstrating that this cross-modal plasticity can be observed at the level of *in vivo* responses to sensory stimulation. This cross-modal plasticity is different from that reported in previous studies at the systems and behavioral levels, where deprivation of sensory inputs to one modality often led to compensatory increases in the functionality of nondeprived modalities[13–16]. Few studies have examined the synaptic basis of cross-modal plasticity. One report showed that dark-rearing of 4-week-old rats for 1 week increased mEPSC amplitudes in V1 and reduced mEPSC amplitudes in S1 (ref. 17). Another study found that visual deprivation of P21 rats for 36 h activated serotonin-mediated signaling and promoted AMPAR insertion in the barrel cortex[18]. We believe that the differences between our results and those of previous studies[17,18] likely arise from differences in when the deprivation procedure is initiated: in previous studies the visual deprivation protocol had been initiated in the third or fourth postnatal week, after the animals had received some normal visual experience, whereas we started our sensory deprivation and/or enhancement manipulations at birth, before the onset of sensory experience. We also assayed the effects of sensory experience on synaptic transmission earlier than previous studies.

Why might there be a different form of cross-modal plasticity during early development? We surmise that this might be due to lower activity early in development, while neurons grow and form connections. The generation of neuronal activity, in the form of either electrical activity or diffusible trophic factors, is itself dependent on initial neural circuit wiring and synapse formation. Thus, for developing sensory cortices, all forms of sensory experience need to first work together to promote development of cortical circuitry. Later on, when there is more activity overall, other Hebbian and homeostatic mechanisms[12,17,18] join in to refine the circuit.

We found that cross-modal effects of whisker deprivation and dark rearing can be detected (**Supplementary Fig. 1**) as early as P7, demonstrating early onset of this form of experience-dependent cross-modal plasticity. Consistently, previous work has shown that responses to visual stimuli can be detected through the closed eyelid long before eye opening[41]. As critical periods for different brain regions occur at different times[42], the lack of cross-modal plasticity in the PFC at P14 may be due to this brain region having a different developmental time course as compared to the sensory cortices.

One might ask whether an additive effect of sensory experience on excitatory synaptic transmission would eventually lead to too much excitation and thus instability of the circuit. We found that sensory deprivation led to reduced excitatory synaptic transmission and no changes in inhibition, resulting in net reduction in neuronal firing, whereas increasing sensory experience through environmental enrichment significantly increased both excitatory and inhibitory synaptic transmission (**Fig. 8** and **Supplementary Fig. 7**). Thus, although excitatory synaptic transmission in the sensory cortices is bidirectionally regulated by sensory experience, inhibition is most sensitive to increased sensory experience. This is consistent with our previous findings in the hippocampus, where we observed increased GABAergic synaptic transmission before detectable changes in glutamatergic synaptic transmission[39].

A new role for oxytocin in cortical development

We identified a role for oxytocin in promoting excitatory synaptic transmission in the sensory cortices, at a much earlier developmental time point than its previously described roles in lactation, in parturition or in mediating social emotional behaviors[23–25]. We found that oxytocin expression in the PVN, as well as oxytocin peptide level in

the sensory cortices, was bidirectionally regulated by sensory experience. Furthermore, exogenous oxytocin mimicked the effects of sensory experience in promoting excitatory synaptic transmission, and interfering with oxytocin signaling significantly reduced excitatory synaptic transmission. These results raised the questions of (i) how sensory experience affects oxytocin production and secretion in the PVN; (ii) how oxytocin travels from the PVN to the sensory cortices; and (iii) how oxytocin affects excitatory synaptic transmission in the sensory cortices.

In addressing the first question, we showed that sensory deprivation reduced the spontaneous firing rates of oxytocin neurons in the PVN, thus providing a circuit basis for how sensory experience regulated oxytocin expression. In terms of whether sensory experience regulated oxytocin production or secretion, our results suggest that both processes contribute. In terms of production, oxytocin mRNA level, as well as the number of oxytocin-positive neurons in the PVN, was regulated by sensory experience. As we did not detect significant apoptosis under control or sensory deprivation conditions at P14 (**Supplementary Fig. 3c–e**), we believe that the lower number of oxytocin-positive neurons was most likely due to reduced synthesis below detection threshold, although cell death at earlier time points cannot be excluded. We also detected a significant reduction in oxytocin release in acute PVN slices prepared from sensory-deprived mice. Previous studies described a positive feedback loop for oxytocin-dependent oxytocin release, where oxytocin secreted from the somatodendritic compartment acts on OXTR in PVN oxytocin-expressing neurons to increase the activity of these neurons and promote additional release of oxytocin[25,31,43,44]. Thus, under sensory deprivation, reduced oxytocin synthesis and release from the PVN, as well as lower activity of oxytocin neurons, likely contribute additively to reducing the level of oxytocin.

Our observation that sensory deprivation reduced oxytocin release from the PVN began to address how oxytocin travels from the PVN to the sensory cortices. As compared to classic neurotransmitters, which have short half-lives and are effective in the micromolar range, neuropeptides have much longer half-lives and are effective in the low nanomolar concentrations[31]. Dendritic release of oxytocin has been studied extensively and demonstrated to be sufficient to mediate its physiological functions in the central nervous system[30–32]. We also demonstrated the ability of oxytocin to travel long distances in the brain, by showing that exogenous oxytocin injected into S1 cross-modally affected mEPSCs in V1, whereas oxytocin antibodies injected into the lateral ventricle reduced excitatory synaptic transmission in both S1 and V1. Locally released oxytocin can travel by diffusion or via the CSF to reach the sensory cortices. These possibilities are not mutually exclusive, and in fact, the CSF has been proposed to be either the source or sink of oxytocin in the brain[30,33]. In both cases, one would expect to observe reduced level of CSF oxytocin after sensory deprivation, which we indeed observed. Together, the effect of sensory deprivation on reducing oxytocin release from the PVN and in reducing its CSF level, as well as the ability of oxytocin antibody injected into the lateral ventricle to reduce mEPSC frequency, all point to CSF as the primary mode by which oxytocin reaches the sensory cortices.

Our findings suggest that axonally released oxytocin, either via direct projections to the sensory cortices or via the pituitary and secretion into the bloodstream, is unlikely to regulate development of sensory cortices. Evidence includes the inability of oxytocin to cross the blood-brain barrier[34], the lack of change in plasma oxytocin level after sensory deprivation, very different developmental profiles of oxytocin in the sensory cortices and in plasma, and the lack of direct oxytocin projections to the sensory cortices identified in previous studies[25] or through our efforts.

Finally, we discuss how oxytocin regulates excitatory synaptic transmission in the sensory cortices. The significant reduction in excitatory synaptic transmission in *Oxt*$^{-/-}$ mice demonstrates an important role of oxytocin in the normal cortical development. This result is supported by those of functional antibody block and pharmacological experiments. As direct application of oxytocin to S1 brain slices increased mEPSC frequencies over the course of minutes, at least one mechanism by which oxytocin regulates excitatory synaptic transmission takes place rapidly. We demonstrated that this occurred through a postsynaptic mechanism with the following lines of evidence: (i) expression of *Oxtr* siRNA in layer II/III pyramidal neurons reduced mEPSC frequencies and blocked the effect of exogenous oxytocin application; (ii) intracellular BAPTA application to layer II/III pyramidal neurons blocked oxytocin-induced increase in mEPSC frequencies; (iii) oxytocin application increased AMPAR/NMDAR ratio but did not affect paired-pulse ratios; and (iv) *in vivo* oxytocin injection increased GRIA2 level in both S1 and V1.

Physiological implications for cortical development

What is the physiological importance of this oxytocin-mediated experience-dependent cross-modal plasticity? At the simplest level, it iterates the importance of multimodal sensory experience to cortical development. Our results showed that sensory experience, in addition to promoting development of the corresponding sensory cortex, also cross-modally regulated development of other sensory cortices. Extending this further, one would expect young individuals with defects in sensory inputs to benefit from additional stimulations of nondeprived sensory modalities, just as environmental enrichment resulted in significant recovery of excitatory synaptic transmission in the sensory cortex corresponding to the deprived sensory modality.

The cross-modal contributions of other sensory inputs to cortical development are likely to be most physiologically relevant if the sensory deprivation is partial, temporary or reversible. 'Hypersensititivy and hyposensitivity to sensory inputs' has been shown to be prevalent among children with ASD[20,21] and has been added as a diagnostic criterion in the fifth edition of the *Diagnostic and Statistical Manual of Mental Disorders*. As reduced social interaction is a hallmark of autism, the ability of oxytocin to promote trust, empathy, eye contact and face memory[23,24,26–28] has made it a hotly debated therapy for treating children with ASD[23,26–28]. Our results add a new dimension to the picture by showing that oxytocin, in addition to its prosocial roles, also participates in experience-dependent development of the sensory cortices. The effect of oxytocin on cortical development could be one of the mechanisms by which it provides beneficial effects to children with ASD. Furthermore, as multimodal sensory experience can increase the cortical level of oxytocin, at least in animal models, our results suggest the possible use of multimodal sensory stimulation as a potential therapy for young children with altered sensory inputs and/or autistic features.

METHODS

Methods and any associated references are available in the online version of the paper.

Accession codes. Gene Expression Omnibus: GSE53136 (**Supplementary Fig. 2**).

Note: Any Supplementary Information and Source Data files are available in the online version of the paper.

ACKNOWLEDGMENTS

We thank S. Young (US National Institute of Mental Health) for the oxytocin knockout mice, V. Grinevich (Max Planck Institute, Heidelberg, Germany) for the AAV-OXT-Venus construct, Y. Lu, X. Zeng and S. He for technical assistance, and colleagues at ION and members of the Yu laboratory for suggestions and comments. This work was supported by grants from the Ministry of Science and Technology (2011CBA00400) to X.Y. and H.Y., the National Natural Science Foundation of China (31125015 and 31321091) to X.Y., the China Postdoctoral Science Foundation (2013M540393) and Postdoctor Research Program of Shanghai Institutes for Biological Sciences, Chinese Academy of Sciences (2013KIP306) to S.-J.L.

AUTHOR CONTRIBUTIONS

J.-J.Z., S.-J.L. and X.Y. designed the study and wrote the paper. J.-J.Z. performed and analyzed all *in vitro* electrophysiology experiments; S.-J.L. performed and analyzed biochemistry and immunohistochemistry experiments, with the help of W.-Y. M. and X.-D.Z.; X.-D.Z. performed stereotaxic injections with the help of J.-J.Z.; D.Z. performed *in vivo* electrophysiology experiments; D.Z. and H.Y. analyzed *in vivo* electrophysiology experiments. All authors edited the paper.

COMPETING FINANCIAL INTERESTS

The authors declare no competing financial interests.

1. Katz, L.C. & Shatz, C.J. Synaptic activity and the construction of cortical circuits. *Science* **274**, 1133–1138 (1996).
2. Crair, M.C. Neuronal activity during development: permissive or instructive? *Curr. Opin. Neurobiol.* **9**, 88–93 (1999).
3. Sur, M. & Rubenstein, J.L. Patterning and plasticity of the cerebral cortex. *Science* **310**, 805–810 (2005).
4. Wiesel, T.N. Postnatal development of the visual cortex and the influence of environment. *Nature* **299**, 583–591 (1982).
5. Fox, K. Anatomical pathways and molecular mechanisms for plasticity in the barrel cortex. *Neuroscience* **111**, 799–814 (2002).
6. Feldman, D.E. & Brecht, M. Map plasticity in somatosensory cortex. *Science* **310**, 810–815 (2005).
7. Fox, K. & Wong, R.O. A comparison of experience-dependent plasticity in the visual and somatosensory systems. *Neuron* **48**, 465–477 (2005).
8. Espinosa, J.S. & Stryker, M.P. Development and plasticity of the primary visual cortex. *Neuron* **75**, 230–249 (2012).
9. Nithianantharajah, J. & Hannan, A.J. Enriched environments, experience-dependent plasticity and disorders of the nervous system. *Nat. Rev. Neurosci.* **7**, 697–709 (2006).
10. Sale, A., Berardi, N. & Maffei, L. Enrich the environment to empower the brain. *Trends Neurosci.* **32**, 233–239 (2009).
11. van Praag, H., Kempermann, G. & Gage, F.H. Neural consequences of environmental enrichment. *Nat. Rev. Neurosci.* **1**, 191–198 (2000).
12. Feldman, D.E. Synaptic mechanisms for plasticity in neocortex. *Annu. Rev. Neurosci.* **32**, 33–55 (2009).
13. Bavelier, D. & Neville, H.J. Cross-modal plasticity: where and how? *Nat. Rev. Neurosci.* **3**, 443–452 (2002).
14. Bavelier, D., Dye, M.W. & Hauser, P.C. Do deaf individuals see better? *Trends Cogn. Sci.* **10**, 512–518 (2006).
15. Merabet, L.B. & Pascual-Leone, A. Neural reorganization following sensory loss: the opportunity of change. *Nat. Rev. Neurosci.* **11**, 44–52 (2010).
16. Frasnelli, J., Collignon, O., Voss, P. & Lepore, F. Crossmodal plasticity in sensory loss. *Prog. Brain Res.* **191**, 233–249 (2011).
17. Goel, A. *et al.* Cross-modal regulation of synaptic AMPA receptors in primary sensory cortices by visual experience. *Nat. Neurosci.* **9**, 1001–1003 (2006).
18. Jitsuki, S. *et al.* Serotonin mediates cross-modal reorganization of cortical circuits. *Neuron* **69**, 780–792 (2011).
19. He, K., Petrus, E., Gammon, N. & Lee, H.K. Distinct sensory requirements for unimodal and cross-modal homeostatic synaptic plasticity. *J. Neurosci.* **32**, 8469–8474 (2012).
20. Marco, E.J., Hinkley, L.B., Hill, S.S. & Nagarajan, S.S. Sensory processing in autism: a review of neurophysiologic findings. *Pediatr. Res.* **69**, 48R–54R (2011).
21. Suarez, M.A. Sensory processing in children with autism spectrum disorders and impact on functioning. *Pediatr. Clin. North Am.* **59**, 203–214 (2012).
22. Micheva, K.D. & Beaulieu, C. Quantitative aspects of synaptogenesis in the rat barrel field cortex with special reference to GABA circuitry. *J. Comp. Neurol.* **373**, 340–354 (1996).
23. Insel, T.R. The challenge of translation in social neuroscience: a review of oxytocin, vasopressin, and affiliative behavior. *Neuron* **65**, 768–779 (2010).
24. Lee, H.J., Macbeth, A.H., Pagani, J.H. & Young, W.S. III. Oxytocin: the great facilitator of life. *Prog. Neurobiol.* **88**, 127–151 (2009).
25. Stoop, R. Neuromodulation by oxytocin and vasopressin. *Neuron* **76**, 142–159 (2012).
26. Green, J.J. & Hollander, E. Autism and oxytocin: new developments in translational approaches to therapeutics. *Neurotherapeutics* **7**, 250–257 (2010).
27. Miller, G. Neuroscience. The promise and perils of oxytocin. *Science* **339**, 267–269 (2013).
28. Yamasue, H. *et al.* Integrative approaches utilizing oxytocin to enhance prosocial behavior: from animal and human social behavior to autistic social dysfunction. *J. Neurosci.* **32**, 14109–14117 (2012).
29. Knobloch, H.S. *et al.* Evoked axonal oxytocin release in the central amygdala attenuates fear response. *Neuron* **73**, 553–566 (2012).
30. Landgraf, R. & Neumann, I.D. Vasopressin and oxytocin release within the brain: a dynamic concept of multiple and variable modes of neuropeptide communication. *Front. Neuroendocrinol.* **25**, 150–176 (2004).
31. Ludwig, M. & Leng, G. Dendritic peptide release and peptide-dependent behaviours. *Nat. Rev. Neurosci.* **7**, 126–136 (2006).
32. Leng, G. & Ludwig, M. Neurotransmitters and peptides: whispered secrets and public announcements. *J. Physiol.* **586**, 5625–5632 (2008).
33. Veening, J.G., de Jong, T. & Barendregt, H.P. Oxytocin-messages via the cerebrospinal fluid: behavioral effects; a review. *Physiol. Behav.* **101**, 193–210 (2010).
34. McEwen, B.B. Brain-fluid barriers: relevance for theoretical controversies regarding vasopressin and oxytocin memory research. *Adv. Pharmacol.* **50**, 531–592, 655–708 (2004).
35. Caldwell, H.K., Stephens, S.L. & Young, W.S. III. Oxytocin as a natural antipsychotic: a study using oxytocin knockout mice. *Mol. Psychiatry* **14**, 190–196 (2009).
36. Gimpl, G. & Fahrenholz, F. The oxytocin receptor system: structure, function, and regulation. *Physiol. Rev.* **81**, 629–683 (2001).
37. Tribollet, E., Dubois-Dauphin, M., Dreifuss, J.J., Barberis, C. & Jard, S. Oxytocin receptors in the central nervous system. Distribution, development, and species differences. *Ann. NY Acad. Sci.* **652**, 29–38 (1992).
38. Hammock, E. & Levitt, P. Oxytocin receptor ligand binding in embryonic tissue and postnatal brain development of the C57BL/6J mouse. *Front. Behav. Neurosci.* **7**, 195 (2013).
39. He, S., Ma, J., Liu, N. & Yu, X. Early enriched environment promotes neonatal GABAergic neurotransmission and accelerates synapse maturation. *J. Neurosci.* **30**, 7910–7916 (2010).
40. Huttenlocher, P.R. *Neural Plasticity: The Effects of Environment on the Development of the Cerebral Cortex* (Harvard University Press, 2002).
41. Krug, K., Akerman, C.J. & Thompson, I.D. Responses of neurons in neonatal cortex and thalamus to patterned visual stimulation through the naturally closed lids. *J. Neurophysiol.* **85**, 1436–1443 (2001).
42. Hensch, T.K. Critical period regulation. *Annu. Rev. Neurosci.* **27**, 549–579 (2004).
43. Chevaleyre, V., Dayanithi, G., Moos, F.C. & Desarmenien, M.G. Developmental regulation of a local positive autocontrol of supraoptic neurons. *J. Neurosci.* **20**, 5813–5819 (2000).
44. Ludwig, M. *et al.* Intracellular calcium stores regulate activity-dependent neuropeptide release from dendrites. *Nature* **418**, 85–89 (2002).

ONLINE METHODS

Animals. C57BL/6 mice were used for all experiments. All animal procedures complied with the animal care standards set forth by the US National Institutes of Health and were approved by the Institutional Animal Care and Use Committee of the Institute of Neuroscience, Chinese Academy of Sciences. The P14 group included P13–P15 mice, other ages as stated. Both male and female mice were used. The *Oxt*$^{-/-}$ mice[35] in C57/BL6 background were gifts of S. Young (US National Institute of Mental Health).

Sensory deprivation and enrichment manipulations. In all experiments, control mice were housed in standard plastic cages (32.5 cm × 21 cm × 18.5 cm) with corn bedding, *ad libitum* access to food and water and on a 12 h–12 h light-dark cycle. For the whisker-deprivation protocol, littermates were randomly assigned to the control or whisker-deprivation group. All pups underwent anesthesia (isoflurane, P0–P4 pups were kept in the chamber for 10–20 s longer to achieve appropriate level of anesthesia), and only mice assigned to the whisker-deprivation group had their whiskers trimmed from P0–P3 and plucked every other day from P4 until time of the experiment. For the dark-rearing protocol (dark-rearing), the pregnant dams were randomly placed in a cage completely covered by thick black plastic 1–4 d before delivery, and mice were cared for under dim red light. Mice were dark-reared until time of experiment. The environmental enrichment protocol for neonatal mice was as previously described[39]. C57BL/6 pregnant mice (2 for enrichment, 1 for standard control) were randomly assigned to standard or enriched housing 1–4 d before delivery. The enriched housing consists of a large Plexiglass cage (50 cm × 36 cm × 28 cm) containing objects of various shapes and textures, repositioned daily and completely substituted once per week.

Brain-slice preparation. Brain slices from deeply anesthetized mice (0.14 g/kg sodium pentobarbital) were essentially prepared as previously described[39]. For young mice, brains were rapidly removed and immersed in ice-cold dissection buffer containing (in mM) CholineCl 110, KCl 2.5, NaH_2PO_4 1.3, $MgCl_2$ 7, $CaCl_2$ 0.5, $NaHCO_3$ 25 and glucose 20, bubbled with 95% O_2/5% CO_2, pH 7.4. Coronal slices were cut at 300–350 µm using a Leica Vibratome 3000 microslicer. Brain slices were allowed to recover in a submersion holding chamber with artificial cerebral spinal fluid (aCSF) consisting of (in mM): NaCl 125, KCl 2.5, NaH_2PO_4 1.3, $MgCl_2$ 1.3, $CaCl_2$ 2, $NaHCO_3$ 25 and glucose 20, bubbled with 95% O_2/5% CO_2 for 30 min at 37 °C and an additional 30 min at 25–28 °C before recordings were made. For adult mice, brains were rapidly removed and immersed in ice-cold aCSF. After slicing in aCSF, brain slices were allowed to recover in a submersion holding chamber with solution consisting of (in mM) *N*-methyl-D-glucamin 110, HCl 110, KCl 2.5, NaH_2PO_4 1.2, $MgSO_4$ 10, $CaCl_2$ 0.5, $NaHCO_3$ 25 and glucose 25, bubbled with 95% O_2/5% CO_2 for 15 min at 37 °C and a further 60 min in aCSF at 25–28 °C before recordings. Slices were visualized with a Nikon FN1 microscope and perfused with oxygenated aCSF at a rate of 6–8 ml/min at 25–28 °C. The barrel field of primary somatosensory cortex (S1), primary visual cortex (V1), primary auditory cortex (Au1), frontal association cortex (PFC) and the dorsal anterior region of the paraventricular nucleus of hypothalamus (PVN) were identified according to standard stereotaxic coordinates[45].

Whole-cell electrophysiological recordings. Whole-cell recordings were made from layer II/III pyramidal neurons or oxytocin neurons in the PVN with a MultiClamp 700B amplifier (Molecular Devices). Signals were filtered at 2 kHz and sampled at 10 kHz using Digidata 1332A (Molecular Devices). For mEPSC recordings, glass pipettes (resistance, 3–5 MΩ) were loaded with internal solution containing (in mM) $CsMeSO_4$ 100, CsCl 25.5, HEPES 10, NaCl 8, EGTA 0.25, glucose 10, MgATP 4 and Na_3GTP 0.3 (pH 7.3, 280–290 mOsm), and all neurons were held at −70 mV; 50 µM picrotoxin and 0.5 µM TTX were added to block $GABA_A$ and Na^+ currents, respectively. For mIPSC recordings, a high chloride internal solution containing (in mM) CsCl 110, NaCl 10, $MgCl_2$ 5, EGTA 0.6, MgATP 2, Na_3GTP 0.2 and HEPES 40 was used, and cells were held at −60 mV; 10 µM NBQX and 0.5 µM TTX were added to block AMPA and Na^+ currents, respectively.

For spontaneous firing recordings of cortical neurons, slices were perfused in modified aCSF containing (in mM) NaCl 124, KCl 3.5, NaH_2PO_4 1.25, $MgCl_2$ 0.5, $CaCl_2$ 1, $NaHCO_3$ 26 and glucose 25. For spontaneous firing recordings of oxytocin neurons, slices were perfused in normal aCSF. The internal solution contained (in mM) K-gluconate 110, HEPES 20, KCl 20, $MgCl_2$ 5, EGTA 0.6, MgATP 2 and Na_3GTP 0.2. A small current was injected to adjust the membrane potential to −60 mV for cortical neurons and to −50 mV for oxytocin-expressing neurons.

For evoked EPSC recordings, 50 µM picrotoxin was added to aCSF to block $GABA_A$ synaptic currents. EPSCs were evoked with a bipolar tungsten stimulating electrode placed in layer IV of the barrel cortex. Responses were evoked using a Master-8 pulse generator coupled through an Iso-Flex isolator (A.M.P.I.). Cells were held at −70 mV to record AMPAR-mediated EPSCs and at +40 mV to record NMDAR-mediated EPSCs. EPSC amplitudes were calculated by averaging 10–20 traces and measuring at the peak for the AMPAR-mediated component and 40 ms after the onset for the NMDAR-mediated component.

Series and input resistances were continually monitored throughout all experiments. Data were not included if the series resistance changed by more than 20% during the experiment. Data were analyzed using pClamp 9.2 and MiniAnalysis software (Synaptosoft), and at least 50% of the data were analyzed in a blinded fashion. All salts and drugs were obtained from Sigma or Tocris, except TTX was obtained from the Fisheries Science and Technology Development Company, and oxytocin and vasopressin were obtained from GL Biochem.

***In vivo* electrophysiological recordings in V1.** Mice were sedated with an intraperitoneal injection of chlorprothixene (4 mg/kg) and anesthetized with urethane (1.2 g/kg). The animal was head-fixed in a stereotaxic apparatus, with a stream of O_2 flow over the nose. Body temperature was maintained at ~37 °C with a heating blanket (FHC Inc.). Craniotomy (diameter of 1 mm) was made above the left V1, and the dura was removed.

Recordings were made with silicon linear probes (A1x32-Poly2-5mm-50s-177, NeuroNexus Technologies). The neural responses were amplified and filtered with a Cerebus 96-channel system (Blackrock microsystem). Spike signals were bandpass–filtered at 250–7,500 Hz and sampled at 30 kHz. Spikes were offline sorted with the Offline Sorter (Plexon).

Visual stimuli were presented on a 17" monitor (Dell Model P170SB with refresh rate of 60 Hz and mean luminance of ~40 cd/m^2) placed 7 cm from the right (contralateral) eye. The responses of V1 neurons were measured with sparse-noise stimuli, in which a white or black square (8.6° × 8.6° – 18.6° × 18.6°) was flashed on a gray background at each of the 8 × 8 or 10 × 10 positions in a pseudorandom sequence at an effective frame rate of 30 Hz. Each position was stimulated 100 times.

We binned the spike trains at the stimulus frame rate. Spatiotemporal receptive field of each neuron was obtained by cross-correlating the spike response with the sparse noise stimuli[46]. For each neuron, we computed the variance of the receptive field at each time delay after stimulus onset, and defined a signal-to-noise ratio (SNR) as the ratio of the maximum variance to the mean variance at delays 0.6–1 s after stimulus onset[47]. A cell was included in the analysis if the SNR was >2 (ref. 48). As few neurons responding to black squares had SNR > 2, we only analyzed response to white squares.

To determine whether the response at a stimulus position was significant, we computed baseline activity using the mean response within 0.6–1 s after stimulus onset, and defined a threshold as 5 times s.d. above the baseline. For each stimulus position, the response was considered significant if the peak response was above the threshold[49]. Only those cells showing significant visual response to at least one stimulus position were included in further analysis. For each neuron, we computed the peak firing rate in response to the most effective stimulus position.

***In vivo* stereotaxic injections.** Mice were anesthetized with 0.4 g/kg chloral hydrate. All drugs were dissolved in fluorescent beads (Invitrogen, F8811, 1:100). Control mice were injected equivalent volume of buffer containing fluorescent beads unless otherwise stated. Oxytocin (1 µM, 1–1.5 µl), lentivirus expressing *Oxtr* siRNA (1×10^9 transducing units (TU)/ml, 0.5 µl) or control siRNA (2×10^9 TU/ml, 0.5 µl) were injected into the S1 barrel field (bregma: −0.5 mm; lateral: 2.7 mm; ventral: 0.3 mm) using a stereotaxic instrument (Stoelting Co.) and a syringe pump (Harvard Apparatus), at a speed of 0.2 µl/min. Atosiban (200 ng), (D(CH$_2$)$_5^1$,Tyr(Me)^2,Thr^4,Orn^8,des-Gly-NH$_2^9$)-vasotocin

doi:10.1038/nn.3634

(Bachem H-2908, 200 ng) or oxytocin antibody (Phoenix Pharmaceuticals, Inc. G-051-01, 1 µg) was injected into the lateral ventricle (bregma: −0.3 mm; lateral: 1.3 mm; ventral: 1.7 mm). Denatured oxytocin or oxytocin antibody was prepared by 5 min incubation at 95 °C. For retrograde labeling, 1–1.5 µl cholera toxin subunit B (CTB, 1 mg/ml, Alexa Fluor 488 conjugate, Invitrogen) was injected into S1.

For labeling of oxytocin-expressing neurons, 1 µl adeno-associated virus (AAV, 1×10^{12} TU/ml, packaged by NeuronBiotech) expressing the fluorescent protein Venus from the oxytocin promoter (AAV-OXT-Venus, originally named AAV-OT2.6-Venus[35]; construct gift of V. Grinevich, Max Planck Institute Heidelberg, Germany) was injected into the PVN (bregma: −0.3 mm; lateral: −0.8 mm; ventral: 4.0 mm) at P9 or P10, at a speed of 0.1 µl/min. Mice were reared for an additional 4–6 d before electrophysiological recordings were made.

Sample preparation for biochemistry experiments. Mice were deeply anesthetized with 0.14 g/kg sodium pentobarbital, and brain regions were dissected in ice-cold phosphate-buffered saline according to standard stereotaxic coordinates[45], with the help of a mouse brain slicer matrix (Zivi Instruments). For hypothalamic samples, the combined thalamus and hypothalamus region was used, as no clear boundaries differentiated the two. The dissected tissue was rapidly frozen in liquid nitrogen. Cerebrospinal fluid (CSF) was extracted from P14 anesthetized mice through a glass pipette using a refined cisterna magna puncture technique[50].

Synaptic membrane preparation and immunoblot analysis. Brain samples from S1 or V1 region were homogenized in ice-cold HEPES-buffered sucrose (0.32 M sucrose and 4 mM HEPES, pH 7.4) containing freshly added protease inhibitor cocktail tablets (Roche) and phosphatase inhibitor cocktail tablets (Roche), and centrifuged at 1,000*g* for 10 min to pellet the nuclear fraction. The supernatant was then centrifuged at 10,000*g* for 15 min to yield the membrane fraction. Western blots were carried out according to standard protocols. The following antibodies were used: GRIA2 (Millipore, MAB397, 1:1,000), GRIN2B (Millipore, 06–600, 1:1000) and GAPDH (KangChen, KC5G4, 1:10,000). Validation is provided on the supplier's website for all antibodies used as well as on 1DegreeBio for GRIA2 and GRIN2B. Immunoblots were quantified using ImageJ (US National Institutes of Health) as previously described[39].

Oxytocin mRNA microarray and quantitative PCR. Total RNA was extracted from tissue samples using TRIzol reagent (Invitrogen). Microarray analysis was performed by Shanghai Biotechnology Corporation using the Agilent mouse development microarray 4 × 44k (G2519F-015062), according to the manufacturer's protocols. For quantitative (q)PCR experiments, first-strand cDNA was generated using the M-MLV reverse transcriptase (Promega) according to the manufacturer's protocols. The following primers were used: 5′-CTGCCCAGAACATCATCCCT-3′ (forward) and 5′-TGAAGTCGCAGGAGACAACC)-3′ (reverse) for *Gapdh*; 5′-ATGCGCAAGTGTCTCCCCTGC-3′ (forward) and 5′-GGGCTCAG CGCTCCGAGAA-3′ (reverse) for *Oxt*; 5′-CCGCACAGTGAAGATGACCT-3′ (forward) and 5′-AGCATGGCAATGATGAAGGCAG-3′ (reverse) for *Oxtr*. Real-time qPCR was performed using SYBR Green Master Mix (TaKaRa) on LightCycler 480 (Roche Applied Science). All reactions were performed in triplicate, and the amount of mRNA was calculated by absolute quantitation.

Oxytocin peptide level measurements. Brain tissues were homogenized in ice-cold RIPA buffer containing freshly added protease inhibitor cocktail tablets (Roche) and phosphatase inhibitor cocktail tablets (Roche), and centrifuged at 13,000*g* for 10 min at 4 °C. The total protein concentration of the supernatant was measured using the BCA assay (Pierce), and oxytocin concentration was measured using an ELISA kit (Pheonix Pharmaceutics, EK-051-01), according to the manufacturer's instructions. The resulting value was corrected for tissue weight to obtain an estimate of oxytocin concentration, using the assumption that 20% of total tissue volume is extracellular space[51]. For plasma measurements, blood was collected in tubes containing EDTA (2 mg/ml) as an anticoagulant and aprotinin (0.6 trypsin inhibitory units (TIU)/ml) as a protease inhibitor, and centrifuged at 1,600*g* for 10 min at 4 °C. The top layer (plasma) was collected, and the amount of oxytocin was measured as described above.

Measurement of oxytocin release from the PVN. Mice were deeply anesthetized with 0.14 g/kg sodium pentobarbital, and their brains were rapidly removed. The ventral medial region of each brain was dissected, and acute PVN brain slices (350 µm) were prepared in oxygenated ice-cold CholineCl solution, followed by 30 min incubation in aCSF at 36–37 °C. Three PVN slices were then placed in a small chamber containing 150 µl aCSF at 26–28 °C. After secretion reached an equilibrium, samples were collected every 5 min for 20 min as previously described[43,44] and stored at −70 °C for subsequent assay of oxytocin peptide level. Slicing and sample collection were carried out concurrently for pairs of control and sensory-deprived mice.

Immunohistochemistry. Mice were deeply anesthetized with 0.14 g/kg sodium pentobarbital. Intracardial perfusion was performed with phosphate-buffered saline (PBS) followed by 4% paraformaldehyde. Coronal brain sections were cut with a freezing microtome (Leica) at 30 µm. Sections were pretreated in 0.3% hydrogen peroxide for 30 min to block endogenous peroxidase activity and blocked in PBS containing 5% bovine serum albumin and 0.3% Triton X-100 for 1 h at 37 °C, followed by incubation with oxytocin antibody (Phoenix Pharmaceutics, G-051-01, 1:2,500) overnight at 4 °C. After washes, sections were incubated with biotinylated secondary antibodies (1:200, Vector Laboratories) for 45 min at 37 °C, followed by application of avidin-biotin-peroxidase (Vector Laboratories, Vectastain Elite ABC kit, 1:200) for 30 min at 37 °C. Immunoreactivity was visualized with DAB Substrate Kit (Vector Laboratories). Negative controls received the same treatments except that primary antibodies were preblocked with excess amount of oxytocin peptide and showed no specific staining.

For stereological measurements of the number of oxytocin-positive cells in the PVN and SON, every 6th PVN and SON-containing section was selected (a total of six sections per mouse). Images of the complete PVN and SON regions were collected on a Nikon E600FN microscope with a 10× Plan-Apocromat objective. Images were analyzed in a blinded fashion using ImageProPlus software (Media Cybernetics). Pairs of control and sensory-deprived mice were processed together for all steps of the protocol.

To better detect the distribution of oxytocin fibers in the brain, oxytocin immunofluorescence was amplified with the Tyramide Signal Amplification Plus System (TSA Plus Cy3 Kit, NEL 744E001KT, PerkinElmer, Inc.) according to the manufacturer's instructions.

Potential apoptosis of oxytocin neurons in the PVN was examined using the TUNEL assay (Roche, 11684795910). Oxytocin neurons were identified using neurophysin I antibody (Santa Cruz, sc-7810, 1:500). Validation for the antibodies is provided on the supplier's website as well as in **Supplementary Figure 3b**.

DNA constructs and efficiency testing. For the *Oxtr* siRNA construct, the sequence GCTGTGTCGTCTGGTCAAA targeting 330–348 nt of mouse *Oxtr* coding sequence (*Oxtr*-RNAi-1) and sequence GGTCAGTAGTGTCAAGCTT targeting 774–792 nt of mouse *Oxtr* coding sequence *(Oxtr*-RNAi-2) were cloned into the pSuper-EGFP vector. *Oxtr*-RNAi-2 was packaged into the pFUGW-RNAi lentiviral vector by Genechem Co. Ltd., where the siRNA was driven by the *U6* promoter and GFP was expressed from the ubiquitin promoter. Vector for HA-tagged OXTR was generated by inserting the full-length mouse *Oxtr* coding sequence (NM_001081147, 12–1,178 nt) into the pCS2-HA vector. The efficiencies of the *Oxtr* siRNA constructs were tested by transient transfection into HEK 293T cells, followed by western blot analysis. The following primary antibodies were used: HA (Abcam, AB9110, 1:1,000) and GAPDH (KangChen, KC5G4, 1:10,000).

Statistics. For all electrophysiological experiments, unpaired two-tailed Student's *t*-test (for sample pairs) or one-way ANOVA (for three or more samples) followed by Tukey's multiple comparison tests were used. Cumulative distributions were tested against each other using the Kolmogorov-Smirnov two-sample tests. For biochemistry and immunohistochemistry experiments, unpaired *t*-tests were used, except for western blots, where pairs of samples were compared using paired *t*-tests. For comparing three or more conditions, one-way ANOVA was used.

Statistical analyses were carried out using GraphPad Prism 5 (GraphPad Software). Data distribution was assumed to be normal, but this was not formally tested. For electrophysiological experiments, *n* values represent the number of neurons. For all other experiments, *n* values represent the number of mice or litters (when samples from multiple mice were pooled). At least three mice from two or more litters were used for each experimental condition. No statistical methods were used to predetermine sample sizes but our sample sizes are similar to those reported in our previous publication[39] and other publications in the field[17,18,44,52,53]. For immunohistochemistry and *in vivo* electrophysiology experiments, all data were analyzed in a blinded fashion. For *in vitro* electrophysiology experiments, at least 50% of the data were analyzed in a blinded fashion. Data were not collected in a blinded fashion. Results are shown as mean ± s.e.m., and statistical significance was set at $^{*}P < 0.05$, $^{**}P < 0.01$, $^{***}P < 0.001$.

45. Paxinos, G. & Franklin, K.B.J. *The Mouse Brain in Stereotaxic Coordinates* (Academic Press, San Diego, 2001).
46. Jones, J.P. & Palmer, L.A. The two-dimensional spatial structure of simple receptive fields in cat striate cortex. *J. Neurophysiol.* **58**, 1187–1211 (1987).
47. Malone, B.J., Kumar, V.R. & Ringach, D.L. Dynamics of receptive field size in primary visual cortex. *J. Neurophysiol.* **97**, 407–414 (2007).
48. Yeh, C.I., Xing, D. & Shapley, R.M. "Black" responses dominate macaque primary visual cortex v1. *J. Neurosci.* **29**, 11753–11760 (2009).
49. Zhu, Y. & Yao, H. Modification of visual cortical receptive field induced by natural stimuli. *Cereb. Cortex* **23**, 1923–1932 (2013).
50. Liu, L. & Duff, K. A technique for serial collection of cerebrospinal fluid from the cisterna magna in mouse. *J. Vis. Exp.* **21**, 960 (2008).
51. Hrabetova, S. & Nicholson, C. *Biophysical Properties of Brain Extracellular Space Explored with Ion-Selective Microelectrodes, Integrative Optical Imaging and Related Techniques* (CRC Press, 2007).
52. Durand, S. *et al.* NMDA receptor regulation prevents regression of visual cortical function in the absence of Mecp2. *Neuron* **76**, 1078–1090 (2012).
53. Tabuchi, K. *et al.* A neuroligin-3 mutation implicated in autism increases inhibitory synaptic transmission in mice. *Science* **318**, 71–76 (2007).

doi:10.1038/nn.3634